

HEFAT2010
7th International Conference on Heat Transfer, Fluid Mechanics and Thermodynamics
19-21 July 2010
Antalya, Turkey

2D SUPERCRITICAL FREE-SURFACE FLOW: AN EXPERIMENTAL STUDY

A. BOUGAMOZA, T. GUENDOZEN-DABOUZ¹, K. BOUZELHA-HAMMOUM², M. BOUHAEF¹ & T. ZITOUN¹

¹Laboratoire GIENA, Department of Hydraulics, Faculty of Civil Engineering
 University Houari Boumediene of Science and Technology (USTHB)
 B.P. 32 Bab-Ezzouar, 16111 Algiers

ALGERIA

²Faculty of Engineering Sciences UMMTO University
 15000 Tizi-Ouzou

ALGERIA

mbouhadef@usthb.dz; malbouh@yahoo.fr; http://www.usthb.dz

ABSTRACT

The numerical two-dimensional free-surface steady flow of an incompressible inviscid fluid, over an obstacle lying on the bottom of a channel, is examined. The Finite Volume Method is used for a supercritical regime. The results obtained from the numerical method are confronted with those of experiments carried out in a hydraulic channel for various obstacles.

INTRODUCTION

The effect of the shape of the bottom of a hydraulic channel on the free-surface profile has a great importance in fluid dynamics. Indeed, from the mathematical point of view, the free-surface is not a priori known and two boundary conditions, one being nonlinear, must also be satisfied on it. This problem has been investigated by many authors as [1], [2], [3], [4], [5], for example. Unfortunately, few papers, dealing with experimental works, are published ([13], [15]).

In this paper, we consider supercritical flows in a hydraulic channel on the bottom of which lies obstacles of different shape.

We recall, first of all, the mathematical formulation of the nonlinear problem and its resolution by a volume element method.

MATHEMATICAL FORMULATION

Governing equations

We consider the steady 2-D flow of an inviscid incompressible fluid over an obstacle of maximum height \bar{b} lying on the bottom of a channel. Far upstream, the flow is uniform with a constant velocity U and a depth h .

The fluid being incompressible, one can introduce a streamfunction $\bar{\Psi}(\bar{x}, \bar{y})$ such as:

$$(\bar{u}, \bar{v}) = \left(\frac{\partial \bar{\Psi}}{\partial \bar{y}}, -\frac{\partial \bar{\Psi}}{\partial \bar{x}} \right) \quad (1)$$

where \bar{u} and \bar{v} represent respectively the horizontal and the vertical components of the fluid velocity.

Due to the uniformity of the flow, far upstream of the obstacle, the theorem of Lagrange ensures us its irrotationality.

$$\Delta \bar{\Psi} = 0 \quad (2)$$

The fluid being inviscid, it slips on the bottom of the channel which is then a streamline taken as:

$$\bar{\Psi}(\bar{x}, \bar{y}_f) = 0 \quad (3)$$

where $\bar{y}_f(\bar{x})$ denotes the equation of the bottom.

The free-surface $\bar{y}_0(\bar{x})$ is also a streamline. The value of the streamfunction, on it, is determined by the conservation of the flow discharge.

$$\bar{\Psi}(\bar{x}, \bar{y}_0) = Uh \quad (4)$$

In addition to this kinematic condition, we must express the conservation of the energy of the fluid on this free-surface where the pressure is constant (atmospheric pressure). The Bernoulli's equation gives:

$$g\bar{y}_0 + \frac{1}{2}(V^2 - U^2) = gh \quad (5)$$

g is the acceleration due to gravity and V the free-surface velocity.

We note that this dynamic condition is non-linear and that there is no radiation condition downstream, especially for a subcritical regime with surface waves, except that the velocity of the flow and the height of the free-surface must be bounded.

The problem may be non-dimensionalized with respect to the velocity U and the height h by introducing the following variables:

$$(x, y, b, y_f, y_0) = (\bar{x}, \bar{y}, \bar{b}, \bar{y}_f, \bar{y}_0)/h; (u, v) = (\bar{u}, \bar{v})/U; \Psi = \bar{\Psi}/Uh.$$

The equations (2) to (5) are then written as follows:

$$\Delta \Psi = 0 \quad (6)$$

$$\Psi(x, y_f) = 0 \quad (7.1)$$

$$\left(\frac{\partial}{\partial n}\right)_{y_0} = \sqrt{1 + \frac{2}{F^2}(1 - y_0)} \quad (7.2)$$

$$\Psi(x, y_0) = 1 \quad (7.3)$$

where $F = U/\sqrt{gh}$ is the far upstream Froude number and \bar{n} the outward normal vector.

Experiments carried out in channels show that, according to the value of the Froude number, the free-surface has the aspect of:

- a unique elevation over the obstacle then gradual going back to the undisturbed level ($y_0 = 1$) for a supercritical flow upstream ($F > 1$).
- a depression in the vicinity of the obstacle followed or not by surface waves for a subcritical flow ($F < 1$).

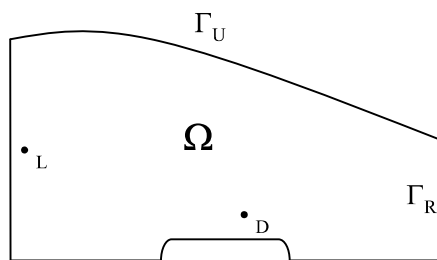


Figure 1 Sketch of the domain

The problem is therefore, in the domain \bullet , described by the equation (6) and boundary conditions (7.1) on \bullet_D , (7.2) and (7.3) on \bullet_U and that of uniformity of the velocity upstream:

$$\Psi = y \quad \text{on } \Gamma_L \quad (7.4)$$

$$\partial\Psi/\partial x = 0 \quad \text{on } \Gamma_L \quad (7.5)$$

The relations (7.2) and (7.3) are known as, respectively, dynamic and kinematic condition. The existence of these two free-surface boundary conditions allows us to consider two iterative processes: associate (7.3) to the problem and then determine the free-surface position verifying (7.2) or the inverse. Due to the fact that our experiments are carried out in a hydraulic channel for a supercritical regime ($F > 1$), we use the second approach because a simple example [14], shows that is stable.

Let us denote M the actually point on the free-surface, N the point just beneath it and M' the determined new location verifying the condition (7.3), for which we choose a linear extrapolation:

$$[\psi(N) - \psi(M)] y(M') = [1 - \psi(M)] y(N) - [1 - \psi(N)] y(M) \quad (8)$$

As we mentioned it in [14], the stream function $\psi(x,y)$ and the free-surface $y_0(x)$ are finally the solution of two problems P_1 and P_2 . The problem P_1 consists on determining $\psi(x,y)$, which is solution of the preceding system of equations, for a known free-surface $y_0(x)$. The problem P_2 allows the determination of a new free-surface location, i.e. $y_0(x)$, solution of the equation (8).

Numerical results

The finite volume method is applied for the resolution of the Laplace equation for the streamfunction \bullet .

For this, it is expressed in a conservative form [14], [16]:

$$\bullet \bullet = \text{div}[\mathbf{F}(\bullet)] = 0 \quad (6)$$

with : $\mathbf{F} = \text{grad}\bullet \quad (9)$

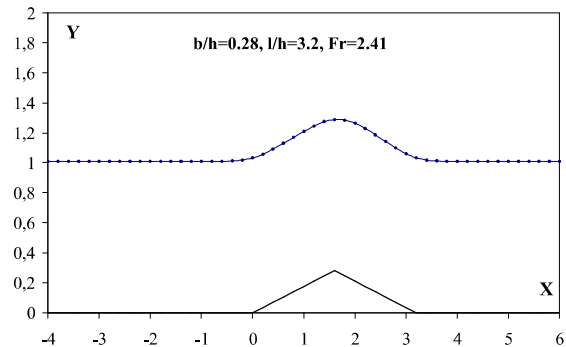


Figure 2 Free-surface profile calculated for a triangle

The figure 2 shows the free-surface profile obtained for a triangular obstacle of height 0.28 at a Froude number $F = 2.41$ corresponding to the experimental data.

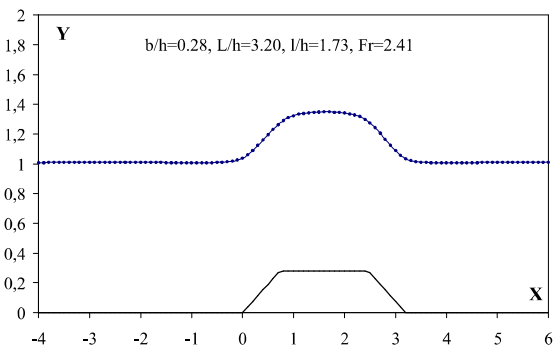


Figure 3 Free-surface profile for a trapezoidal obstacle

The figure 3 is similar to the preceding one but for a trapezoidal obstacle with the same height and Froude number.

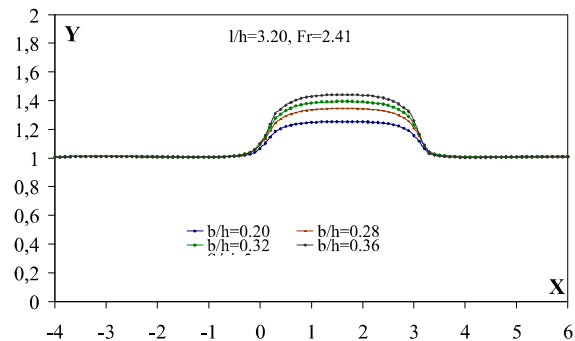


Figure 4 Theoretical free-surface profiles for steps of various heights

The figure 4 shows the evolution of the free-surface profile for a given Froude number and step length with the obstacle height.

EXPERIMENTAL PROCEDURE

The experiments were carried out in a Plexiglas rectangular channel (see [19]) of uniform section (width $a = 7.5$ cm and length $L = 6$ m) allowing a complete visualization of the flow (Photo.1).



Photo 1 View of the hydraulic channel

The upstream supercritical regime is generated by the addition of a convergent (nozzle). It consists on a flexible PVC sheet which thickness is 3 mm and 80 cm length; it is placed so as it gradually directs the flow towards a narrowed exit (Photo 2). The distance between the entry of the channel and the end of the convergent is selected so as to reach a fully supercritical regime slightly disturbed. Indeed, we reduce the cross section of the flow to a narrowed exit opening $H = 2.5$ cm to allow great velocities. The perfect rigidity of the canal is provided by a box girder. The water supply is provided by a horizontal axis closed-circuit pump. The flow control is done by a manual valve which allows the variation of the water discharge. The measurement is made using a flowmeter.

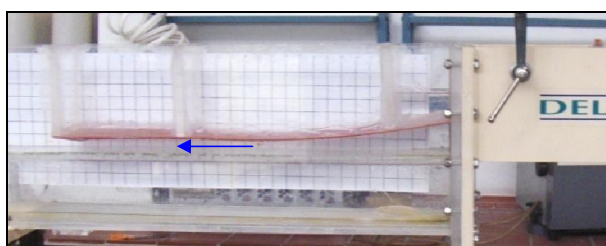


Photo 2 The hydraulic channel with a convergent at the entry

To fix the upstream depth H , we change the discharge Q from $2 \text{ m}^3/\text{h}$ to $16 \text{ m}^3/\text{h}$, with a step of $2 \text{ m}^3/\text{h}$, and this for each Froude number Fr from 2 to 10. The various values of H are given by the relation (10) [20].

$$H = 2.6 \left(\frac{Q}{Fr} \right)^{2/3} \tag{10}$$

We used several types of obstacles of width $a = 7.5$ cm, but with different shapes and lengths: the first rectangular obstacle is 8 cm length and variable maximum thickness; the second obstacle has a trapezoidal shape with a maximum thickness $s = 7$ mm and length $l = 8$ cm; the third obstacle has a symmetrical triangular shape with a maximum thickness $s = 7$ mm and a length $l = 8$ cm.

A liquid level recorder is used to measure the various free-surfaces obtained.

A 1D Laser Doppler Anemometer (Flowlite of DANTEC Dynamics) is also used to measure velocity profiles at various sections of the channel, downstream and upstream of the obstacles (photo 3).

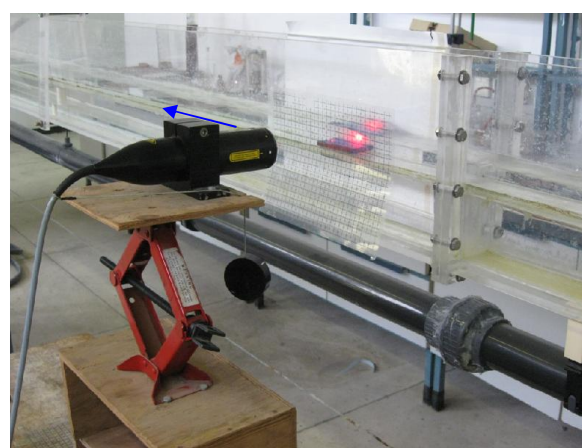


Photo 3 The hydraulic channel with a velocimeter

EXPERIMENTAL RESULTS

Free-surface profiles

We have tested three obstacles with different shapes. The first one, which is identical to that of [20], is triangular.

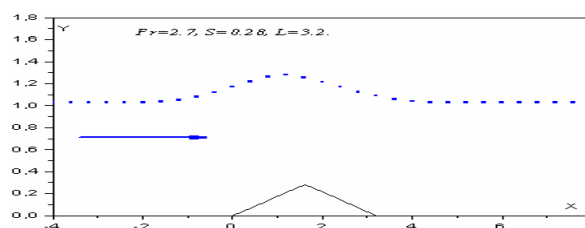


Figure 5 Measured free-surface profile for a triangular obstacle

We remark on the figure 5 ($Fr = 2.7$, $S = s/h = 0.28$, $L = l/h = 3.2$) that, as for the obtained numerical results, the quasi symmetry of the free-surface profile and the horizontality of the level far downstream and far upstream of the obstacle.

The figure 6 shows an identical shape of the free-surface profile for a localised step ($Fr = 2.7$, $S = 0.28$, $L = 3.2$).

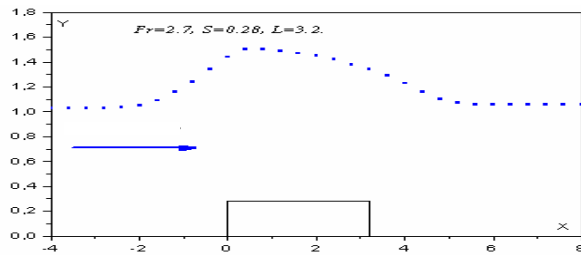


Figure 6 Measured free-surface profile for a step

The figure 7 is relative to a symmetrical trapezoidal obstacle ($Fr = 2.7$, $S = 0.28$, $L = 3.2$)

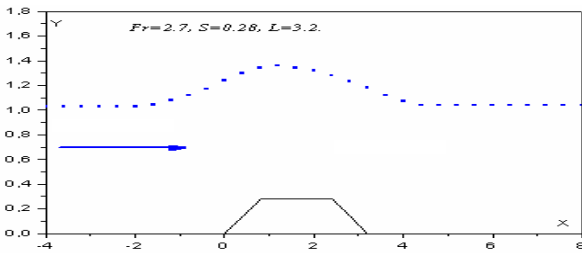


Figure 7 Measured free-surface profile for a trapezoidal obstacle

When we vary the obstacle's thickness ($S = 0.2$ to $S = 0.44$), the allures of the free-surface profiles, for a given Froude number ($Fr = 2.7$), are represented on the figure 8 for steps with the same length and water upstream depth.

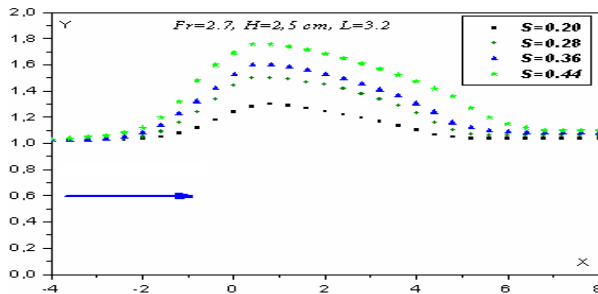


Figure 8 Measured free-surface profiles for steps of same length and various thicknesses

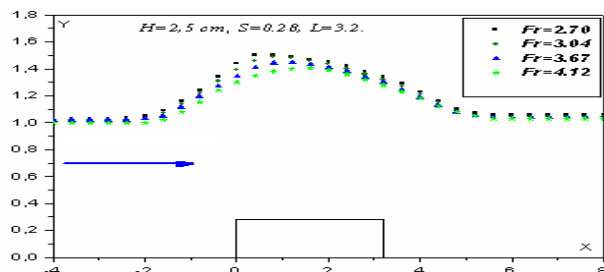


Figure 9 Free-surface profiles at various Froude numbers

For a given step and water upstream depth, the free-surface profile doesn't highly vary with the Froude number as it is shown on the figure 9. The higher is the Froude number, the weaker is the maximum free-surface height.

Velocity profiles

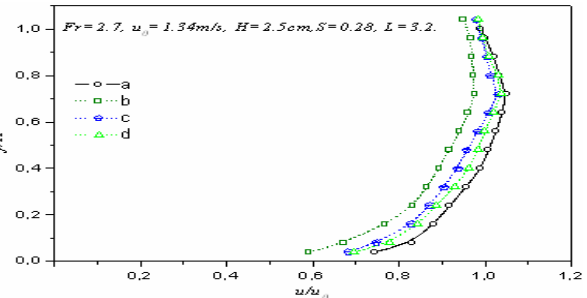


Figure 10 Velocity profiles for different obstacles

The figure 10 shows the different velocity profiles obtained with a LDA velocimeter. The graph (a) is relative to a far upstream section. The graphs (b), (c) and (d) correspond to a far downstream section of a triangular obstacle, a trapezoidal obstacle and a step respectively.

Let us recall that, in the mathematical formulation, the fluid is assumed inviscid and, thus, the velocity profile is uniform and constant far upstream.

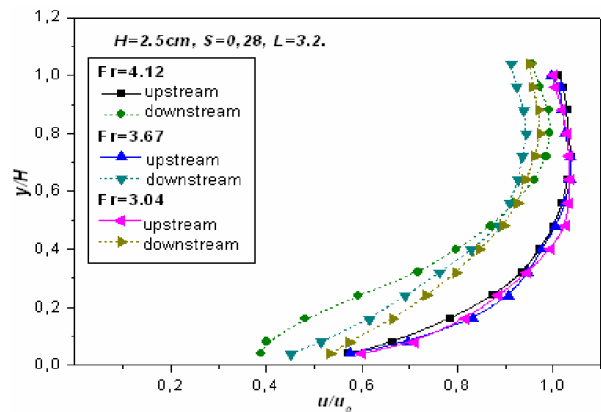


Figure 11 Velocity profiles for a step at various Froude numbers

The velocity profiles represented on the figure 11 show that their shape is very similar at different Froude numbers and depends only on the position of the section (upstream or downstream).

If we change the shape of the obstacle, we remark that the velocity profile varies highly with it for a given section. Indeed, as figure 12 shows it, the profiles are different even if they correspond, for a given Froude number, to the same section located above the obstacle.

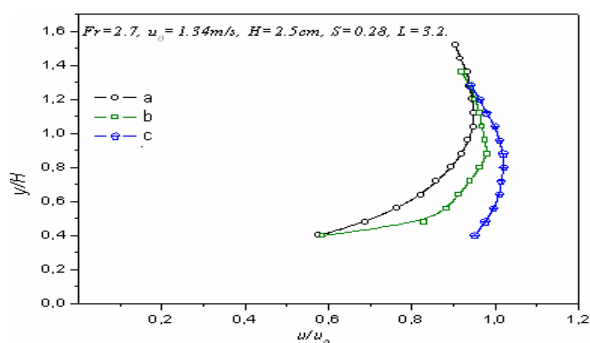


Figure 12 Velocity profiles above a triangle, a trapezoidal obstacle and a step

CONCLUSION

The experimental study which was carried out shows the symmetry which exists between the upstream and the downstream free-surface of a flow for a mode everywhere torrential.

We did not proceed to comparisons between numerical calculation and the experimental values for several reasons: for example, the assumed conditions in the mathematical formulation (inviscid fluid, 2D flow and uniform velocity profile far upstream) are not verified in the experiment, the measurements are carried out in the centre of the hydraulic channel, the Froude number is defined from the volume discharge, and so on.

REFERENCES

- [1] H. Lamb. Hydrodynamics. Cambridge University Press, 1932.
- [2] L.K. Forbes and L. W. Schwartz. Free-surface flow over a semicircular obstruction. *J. Fluid Mech.* 114, 299, 1982.
- [3] Y.Z. Boutros, M.B. Abdelmalek et S.Z. Massoud, Linearized solution of a flow over a non uniform bottom, *J. of Comput and Appli Math*, 16, 105, 1986.
- [4] A.C. King and M.I.G. Bloor. Free-surface flow over a step. *J. Fluid Mech.* 182, 193, 1987.
- [5] M. Amara and M. Bouhadeh. A new approach of numerical modelling of 2D surface waves induced by an obstacle. *Computer Meth. and Water Ress.* C. M. P., 1991.
- [6] P.A. Milewski and J.-M. Vanden-Broeck. Time-dependent gravity-capillary flows past an obstacle. *Wave Motion.* 29, 63-79, 1999.
- [7] B.M. Savage and M.C. Johnson. Flow over ogee spillway: physical and numerical model case study. *J. Hydr. Eng.* 640-649, August 2001.
- [8] D. Boukari, R. Djouadi, D. Teniou, Free-surface flow over a rand obstacle. Theoretical study of the torrential case. *Abstract and Applied Analysis*, 6 (7), pp413-429, 2001
- [9] J.-M. Vanden-Broeck and F. Dias. Steady two-layer flows over an obstacle *Phil. Trans. R. Soc. A* 360, 2137-2154, 2002.
- [10] V. I. Bukreev, Supercritical flow over a sill in an open channel, *Journal of Applied Mechanics and Technical Physics*, Vol. 43, No. 6, pp. 830, 835, 2002.
- [11] V. Guinot, Numerical methods for differential equations, *Hydroinformatics*, 2002.
- [12] V. I. Bukreev, A. V. Gusev. Waves behind a step in an open channel. *Journal of Applied Mechanics and Technical Physics*, 44, N°1, 52-58, 2003.
- [13] M. Bouhadeh, T. Zitoun and T. Guendouzen. Contribution to numerical and experimental study of 2D free-surface flow. *IASME Transactions Journal*, Issue 3, volume 1, pp 455, 459, July 2004.
- [14] M. A. Sarker, D. G. Rhodes. Calculation of free-surface profile over a rectangular broad-crested weir. *Flow Measurement and Instrumentation*, 15, 215-219, 2004.
- [15] K. Bouzelha-Hammoum, M. Bouhadeh and T. Zitoun. Numerical study of 2D free-surface waveless flow over a bump. *WSEAS Transactions on Fluid Mechanics*, Issue 6, volume 1, pp 732, 737, June 2006
- [16] V. Yu. Liapidevskii and Z. Xu, Breaking of waves of limiting amplitude over an obstacle, *Journal of Applied Mechanics and Technical Physics*, Vol. 47, No. 3, pp. 307-313, 2006.
- [17] K. Bouzelha, Contribution à l'étude des écoulements à surface libre : modélisation numérique en théorie non linéaire par la méthode des volumes finis et étude expérimentale, *Thèse de Doctorat d'état*, Univ. Tizi-Ouzou, Algérie, 2007.
- [18] D. Teniou, Sur l'écoulement d'un fluide dans un canal avec obstacle au fond, *Annales Mathématiques Blaise Pascal*, Volume 14, n°2, p. 255-265, 2007.
- [19] V. Yu. Liapidevskii and K. N. Gavrilova, Dispersion and blockage effects in the flow over a sill. *Journal of Applied Mechanics and Technical Physics*, Vol. 49, No. 1, pp. 34-45, 2008.
- [20] K. Bouzelha-Hammoum, M. Bouhadeh, T. Zitoun & T. Guendouzen-Dabouz, Contribution to the study of a free-surface supercritical flow above an obstacle: theory – laboratory work, *International Conference on Fluid Mechanics and Aerodynamics*, Rhodes, 2008.